Magnetic topological transition in transmission line metamaterials

Alena V. Shchelokova, Dmitry S. Filonov, Polina V. Kapitanova, and Pavel A. Belov
ITMO University, St. Petersburg 197101, Russia
(Received 30 June 2014; published 30 September 2014)

We study the magnetic topological transition of the isofrequency curves in the wave vector space from a closed ellipsoid to an open hyperboloid in a metamaterial based on artificial transmission lines. In the radio frequency band we directly measure the emission pattern of a point source placed in the center of the lattice and demonstrate the elliptical wave fronts below the topological transition frequency and hyperbolic wave fronts above the topological transition frequency.

DOI: 10.1103/PhysRevB.90.115155 PACS number(s): 81.05.Xj, 78.67.Pt, 84.40.−x, 41.20.Jb

I. INTRODUCTION

Hyperbolic metamaterial, being a particular class of indefinite media, is a uniaxial system, where the transverse ($\varepsilon_\perp$) and longitudinal ($\varepsilon_\parallel$) components of effective permittivity tensor have opposite signs [1]. Unusual properties of such metamaterials are due to the hyperbolic isofrequency surfaces in the wave vector space [1–5]. Among them are the near field control [6,7], negative refraction, similar to the case of double-negative materials [8–10], the large density of states [11–15], and partial focusing [16]. Hyperbolic metamaterials have been demonstrated for hyperlensing [17] and directional single photon emission [18].

A transition in the topology of the isofrequency surface from a closed ellipsoid to an open hyperboloid by use of artificially nanostructured metamaterials has been described in Ref. [11]. The increased rate of spontaneous emission of emitters positioned near the metamaterial have been demonstrated in the hyperbolic regime. Thus altering the topology of the isofrequency surface by using metamaterials provides a fundamentally new route to manipulate light-matter interactions.

In optical frequency domain the most common implementations of hyperbolic metamaterials are based on layered metal-dielectric structures [11] or arrays of metallic nanowires [19]. For investigation of dielectric properties (complex refractive index or dielectric function) ellipsometry can be used [20]. Ellipsometry is an indirect method, and measured data can not be converted directly into the optical constants of a metamaterial sample; normally a model analysis must be performed. On the other hand the scalability of Maxwell's equations with respect to the operation frequencies enables the investigation of certain phenomena at much lower frequencies, where the fabrication and measurements are more straightforward.

Recently, it has been demonstrated that a metamaterial with a hyperbolic isofrequency curve can be mimicked by two-dimensional transmission lines [21]. It was experimentally confirmed that the emission pattern of a current source has a cross form, that is a fingerprint of hyperbolic media. In this paper we apply the transmission line approach to design and investigate two-dimensional metamaterial with magnetic topological transition. We propose an improved design of the transmission line unit cell to obtain a metamaterial with transition between elliptic and hyperbolic isofrequency curves. We analytically study the topological transition in metamaterial and visualize the allowed propagation directions in elliptic and hyperbolic regimes via investigation of the Green function. To this end we fabricate a prototype of two-dimensional metamaterial using chip components mounted on a printed circuit board and directly measure the emission of an external localized source in the prototype demonstrating the elliptical wave fronts below the resonant frequency and hyperbolic wave fronts above the resonant frequency.

II. MAGNETIC TOPOLOGICAL TRANSITION IN TWO-DIMENSIONAL METAMATERIAL

In this paper we study the magnetic topological transition of the isofrequency curve from a closed ellipsoid to an open hyperboloid [Fig. 1(a)] in a two-dimensional uniaxial metamaterial characterized by scalar permittivity ε and longitudinal and transverse permeabilities μ_x and μ_y. In particular, dispersion equation for a TE-polarized wave, propagating in the x-y plane (magnetic field is oriented along the z axis), reads [3,4]:

$$\frac{k_x^2}{\omega^2\mu_y\varepsilon}+\frac{k_y^2}{\omega^2\mu_x\varepsilon}=1\,, \tag{1}$$

where k_x and k_y are the x and y components of the propagation vector and ω is the frequency. We consider the situation when the permeability tensor component μ_y is frequency independent and component μ_x has a resonant frequency behavior [Fig. 1(b)]. According to Eq. (1) below the resonance frequency where $\mu_x, \mu_y > 0$ the wave propagation is allowed in both x and y directions and the isofrequency curve has a closed form of ellipse. On the other hand, an extreme modification of the isofrequency curve into an open hyperboloid occurs above the resonance frequency where the permeabilities show the opposite signs $\mu_x < 0$ and $\mu_y > 0$.

A high-performance metamaterial can be designed to achieve the required permittivity and permeability responses in the radio frequency range using artificial two-dimensional transmission lines [6,21–24]. To understand the close analogy between electromagnetic wave propagation in an anisotropic medium [described by Eq. (1)] and current and voltage in a transmission line metamaterial, we consider a basic unit cell of a two-dimensional transmission line metamaterial [21] as a symmetric T-circuit composed of serial admittances Y_x and Y_y in x and y directions and a shunt impedance Z. The voltage at one node in the grid is related to its neighbors via the Kirchhoff

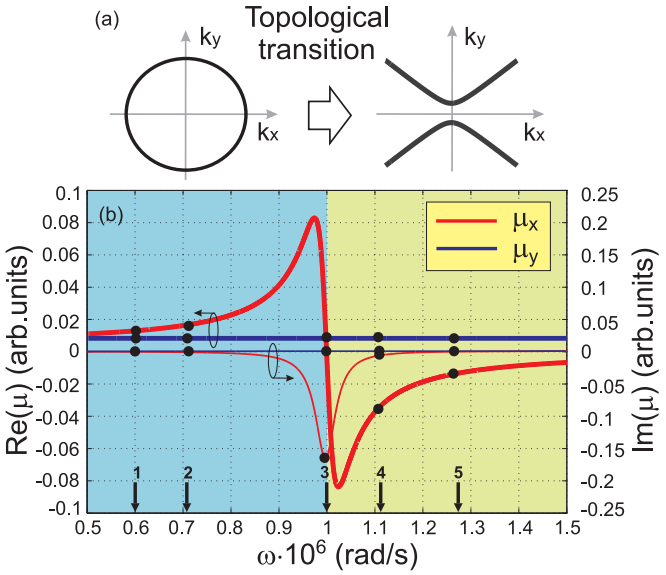

FIG. 1. (Color online) (a) Topological transition between elliptic and hyperbolic isofrequency curves. (b) Permeabilities of a two-dimensional uniaxial metamaterial with magnetic topological transition.

current law:

$$Y_x(U_{x-1,y} + U_{x+1,y}) + Y_y(U_{x,y-1} + U_{x,y+1}) - 2U_{x,y}(Y_x + Y_y) = U_{x,y}/Z\,. \quad (2)$$

To derive the dispersion equation for the structure composed of infinite number of unit cells with $d \times d$ dimension, we can look for a Bloch solution of the form $U_{x,y} = U_0 \exp[i(k_x d + k_y d)]$ and get:

$$Y_x \sin^2(k_x d/2) + Y_y \sin^2(k_y d/2) = -1/(4Z)\,. \quad (3)$$

Assuming the delays per unit cell are small ($k_x d \ll 1, k_y d \ll 1$), we compare Eqs. (1) and (3) to define the relationship between the effective medium parameters and its radio frequency counterparts:

$$\frac{\mu_x}{\mu_y} = \frac{Y_x}{Y_y}\,. \quad (4)$$

From Eq. (4) one may conclude that the shape of the isofrequency contour (elliptic or hyperbolic) that depends on the sign of permeabilities μ_x and μ_y is directly related to the sign of the admittances Y_x and Y_y. The transmission line metamaterial with elliptic isofrequency contours, where the admittances Y_x and Y_y have been implemented as inductances, has been demonstrated in Ref. [24]. In Ref. [21] the transmission line metamaterial with hyperbolic isofrequency contours has been reported, utilizing capacitances as admittances Y_x and inductances as Y_y.

To mimic the metamaterial with magnetic topological transition we improve the unit cell design providing a possibility to change the sign of admittance in one of the directions (see inset Fig. 3). The main difference of the proposed unit cell from the unit cells described in Refs. [24] and [21] is the use of parallel $L_y C_y$ connections in the y direction instead of a single component—inductance or capacitance depending on the desired shape of the isofrequency curve (elliptic or hyperbolic). For the parallel $L_y C_y$ connections we can determine a resonant frequency where the admittance $Y_y = i\omega C_y + 1/i\omega L_y$ changes the sign as $\omega_0 = 1/\sqrt{L_y C_y}$. Below the frequency ω_0 the admittance Y_y has an inductive behavior while above the resonant frequency the capacitive behavior dominates. Thus we are able to get an inductive or capacitive behavior of the unit cell y branch by sweeping the frequency.

III. VISUALIZATION OF MAGNETIC TOPOLOGICAL TRANSITION VIA GREEN FUNCTION

Allowed propagation directions in elliptic and hyperbolic regimes can be directly visualized by the Green function of the metamaterial. The Green function is defined as a voltage distribution induced in the metamaterial by the external localized source. Particularly one has to solve Eq. (2) with the inhomogeneous term $\delta_{x,x_0}(\delta_{y,y_0} - \delta_{y,y_0-1})$ in the right hand side, where x_0 and y_0 are the source coordinates. This corresponds to a voltage of different sign applied to two vertically adjacent lattice nodes.

We demonstrate the evolution of the isofrequency curve and Green function pattern when the frequency sweeps and permeability μ_x changes its value. The characteristic frequencies 1–5 are chosen and marked by dots in Fig. 1(b). The corresponding permeability values are listed in Table I. The value of permeability $\mu_y = 0.008 - 0.0006i$ is constant over the frequency. The isofrequency curves obtained by numerical solution of the dispersion relation (3) are depicted in Fig. 2 in comparison with the simulated spatial distribution of the absolute values of the Green function. The simulation was done for the finite metamaterial sample composed of 31×31 unit cells with the source in the middle node ($x_0 = y_0 = 16$). The values of the unit cell admittances Y_x, Y_y, and Y can be found from the effective medium parameters ε and μ by the following estimations [24]: $i\omega\varepsilon d \to Y$, $i\omega\mu_y d \to Y_x$, $i\omega\mu_x d \to Y_y$, where d is the unit cell dimension. In our case the resonant frequency is $\omega_0 = 10^6$ rad/s (marked by dot 3 in Fig. 1), the effective medium parameters are $\epsilon = 2.7510^{-7}$, $\mu_{x_3} = -0.1677i$, $\mu_y = 0.008 - 0.0006i$, and the unit cell dimension is $d = 12$ mm. Assuming $C = -Yi/\omega_0$, $L_x = 1/i\omega_0 Y_x$, and $C_y = Y_y/(i\omega_0) + 1/(\omega_0{}^2 L_y)$ one can calculate the values of lumped elements as $C = 3300$ pF, $C_y = 0.01$ μF, and $L_x = L_y = 100$ μH. At the edges the structure is loaded by resistors with $R = 100$ Ω to provide matching conditions.

In the characteristic points 1 and 2 when the real parts of the permeabilities μ_x and μ_y are positive, the isofrequency curves have the elliptic shapes [Figs. 2(a) and 2(b)]. The Green function patterns for these cases are depicted in Figs. 2(f)

TABLE I. The characteristic parameters.

Characteristic point #	1	2	3	4	5
Frequency, kHz	95	110	160	185	200
$\mathrm{Re}(\mu_x)10^2$	1.3	1.6	0	−2.3	−1.4
$\mathrm{Im}(\mu_x)10^2$	−0.14	−0.19	−16.77	−0.33	−0.13

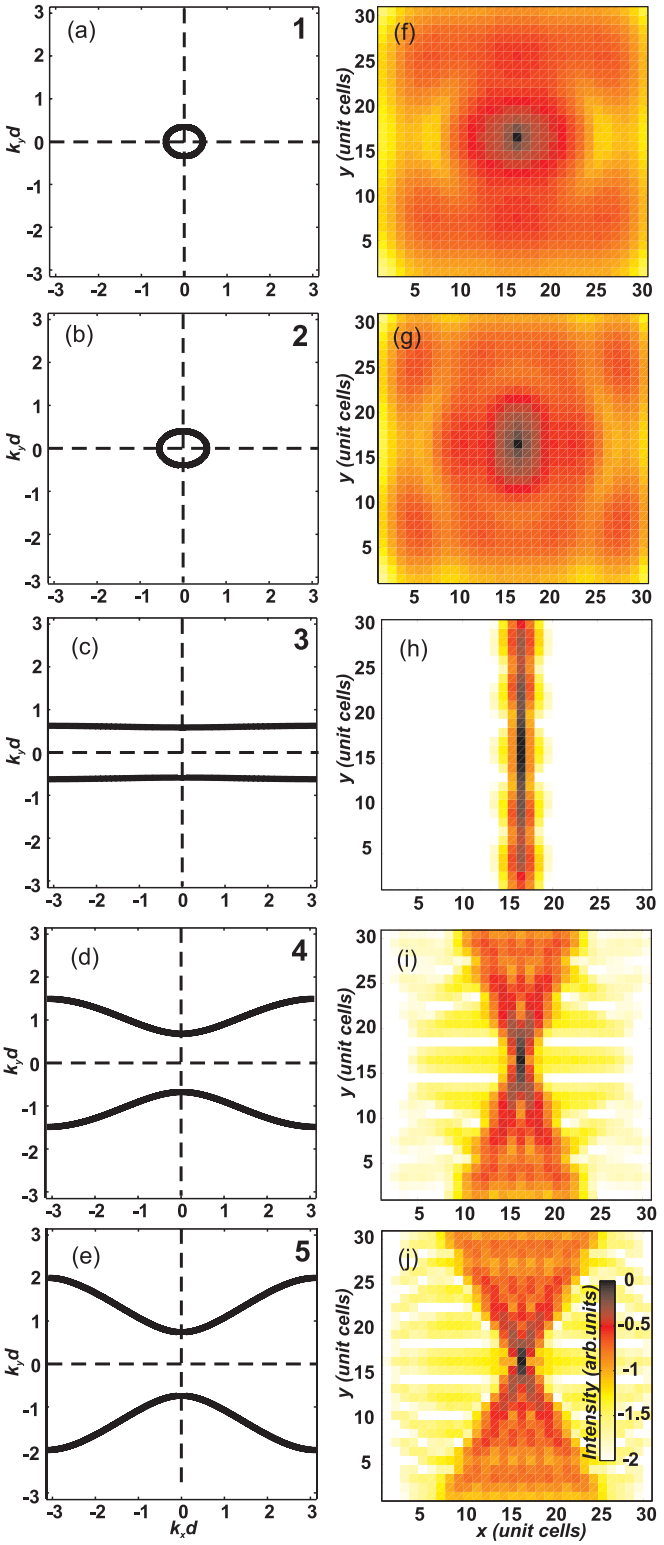

FIG. 2. (Color online) (a)–(e) Isofrequency curves obtained by numerical solution of the dispersion relation (3) for the unit cell parameters: $C = 3300$ pF, $C_y = 0.01$ μF, and $L_x = L_y = 100$ μH. (f)–(j) The simulated spatial distribution of the absolute values of the Green function of the metamaterial composed of 31×31 unit cells at frequencies 1–5, respectively.

and 2(g), respectively. It is clearly seen that the propagation is allowed in all directions. Due to the finite size effects, the patterns are warped instead of circular and have a fourfold rotation symmetry with maxima near the corners of the square. In the characteristic point 3 the real part of μ_x crosses zero and the isofrequency curve is flat [Fig. 2(c)]. As a result the emission is strongly confined along the line $x = x_0$. The isofrequency curves have a hyperbolic form above the resonance when the real parts of permeabilities μ_x and μ_y are of the opposite signs [Figs. 2(d) and 2(e)]. The Green function patterns have the characteristic cross shape [Figs. 2(i) and 2(j)]. The propagation is allowed mainly in the y direction within a narrow cone while a shadow is observed in the x direction. It is important to mention that the cone angle changes with the frequency.

IV. EXPERIMENTAL VERIFICATION OF MAGNETIC TOPOLOGICAL TRANSITION

The prototype of the two-dimensional metamaterial with magnetic topological transition composed of 31×31 unit cells has been fabricated using commercially available chip components mounted on a printed circuit board (Fig. 3). The inductors model LQH32MN101J from Murata have been used as inductances L_x and L_y. We used capacitors model GRM32QR73A103KW from Murata and capacitors model CC1210JKNPO9BN332 from Yageo as capacitances C_y and C_g, respectively. To provide the matching conditions at the edges 100 Ω resistors model ERJ6BQF1R0V from Panasonic have been used. The components have been mounted on a FR4 printed circuit board with permittivity $\varepsilon_r = 4.4$ and a thickness of 1.5 mm. The prototype dimensions are 46 cm×46 cm.

To excite the prototype an arbitrary waveform generator (Keithley 3390) has been connected in the structure center. During the experimental investigation we have directly measured the voltage magnitude in the nodes of the prototype by a digital multimeter (Keithley 270). The Figs. 4(a)–4(e)

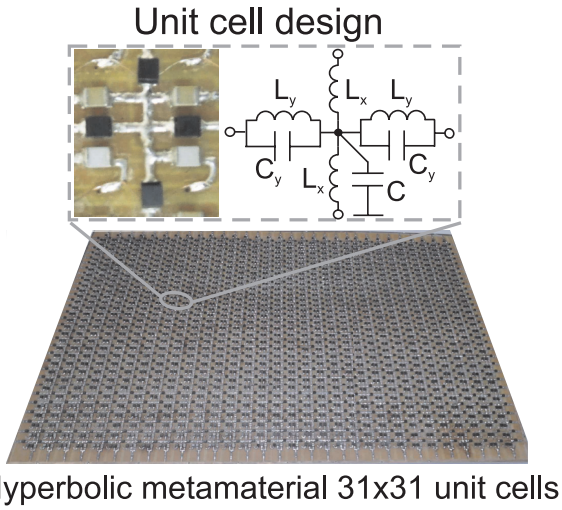

FIG. 3. (Color online) Photograph of the two-dimensional metamaterial prototype fabricated using commercial chip components on a FR4 printed circuit board. The inset shows the unit cell design.

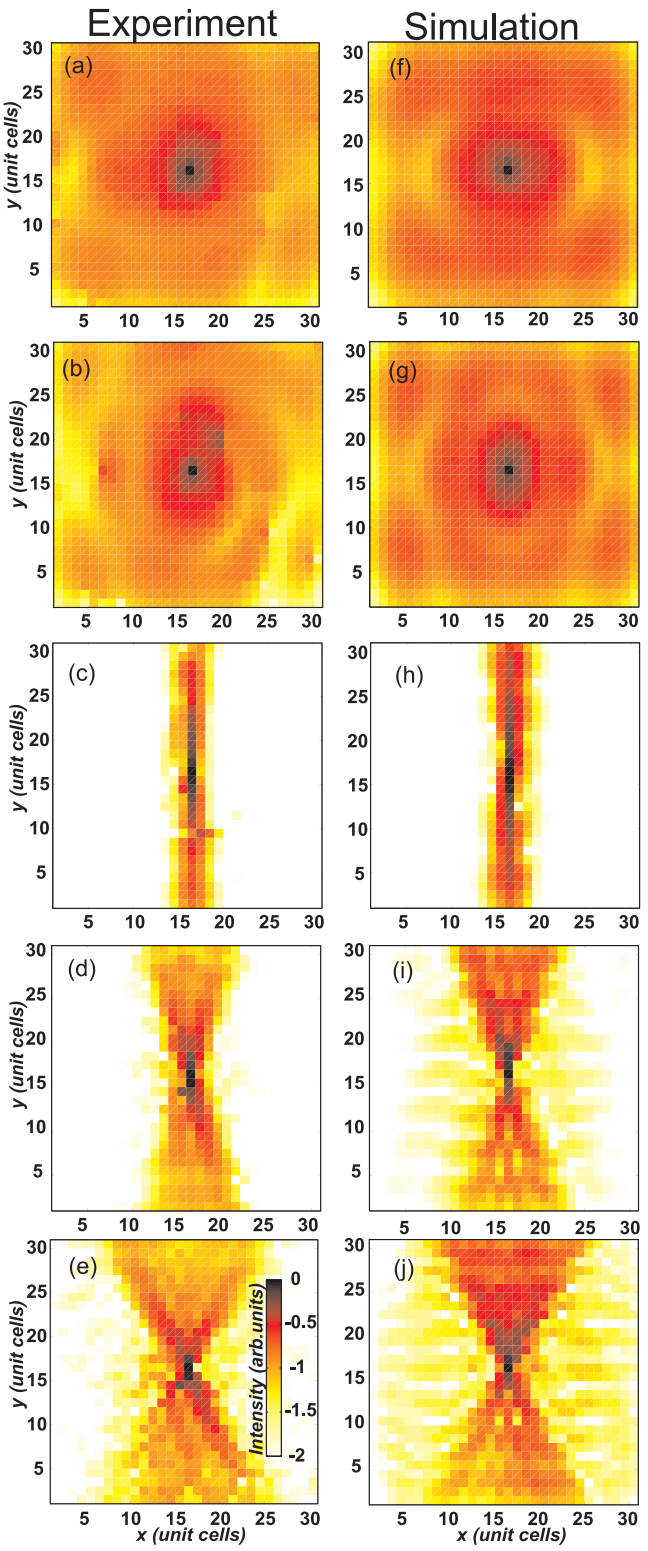

FIG. 4. (Color online) (a)–(e) Measured Green function patterns at frequencies 1–5 in comparison with simulated Green function patterns (f)–(j) in the metamaterial with losses and 10% tolerance of the chip components taken in to account.

represent the measured Green function patterns at the frequencies $f_1 = 95$ kHz, $f_2 = 110$ kHz, $f_3 = 160$ kHz, $f_4 = 185$ kHz, and $f_5 = 200$ kHz which corresponds to the characteristic points 1–5, respectively. As was predicted for the frequencies below the resonance the Green function patterns in the metamaterial structure have an elliptic shape, while at the frequencies above the resonance it becomes hyperbolic. At the frequency of topological transition the measured Green function pattern is singular. Due to the flat isofrequency curve the propagation is allowed only in the y direction.

While the main trends are the same in the measured [Figs. 4(a)–4(e)] and simulated [Figs. 2(f)–2(j)] Green function patterns, a slight asymmetry of the measured patterns in elliptic and hyperbolic regimes is observed. In order to obtain better correspondence between experimental data and the numerical results the loss of chip components and tolerance of their nominal values have been considered. The simulated Green function patterns with losses and 10% tolerance of the chip components taken into account are depicted in Figs. 4(f)–4(j) for the characteristic points 1–5, respectively. We have also noticed that the Green function patterns in the elliptic regime are more stable to the influence of the components tolerance than in the hyperbolic regime. Increase of the components tolerance up to 20% totally destroys the hyperbolic regime.

V. CONCLUSIONS

We have analytically studied, designed, and experimentally investigated the metamaterial with magnetic topological transition from the elliptic to hyperbolic regimes. We have shown that at the frequencies below the resonance the isofrequency curves have an elliptic shape, at the resonance the isofrequency curve is flat, and above the resonance the isofrequency curves have hyperbolic shape. We visualized the allowed propagation directions in the metamaterial via the Green function which was defined as a voltage distribution induced by an external localized source. We have fabricated the metamaterial prototype and experimentally demonstrated this phenomena by direct measurements of the voltage distribution in the metamaterial nodes.

ACKNOWLEDGMENTS

The authors acknowledge useful discussions with A. Poddubny and technical assistance of A. Slobozhanuk and M. Guzhva. Numerical simulations of the transmission line metamaterial were supported by the Russian Science Foundation (Project No. 14-12-00897). The experimental investigation of the prototype was supported by Scholarship and Grant of the President of Russian Federation. A.V.S. and D.S.F. acknowledge the support of the Dynasty Foundation and SPIE Optics and Photonics Education Scholarship.

[1] A. Poddubny, I. Iorsh, P. Belov, and Yu. Kivshar, Nat. Photon. 7, 948 (2013).

[2] D. R. Smith and D. Schurig, Phys. Rev. Lett. 90, 077405 (2003).

[3] I. V. Lindell, S. A. Tretyakov, K. I. Nikoskinen, and S. Ilvonen, Microw. Opt. Tech. Lett. **31**, 129 (2001).
[4] L. Felsen and N. Marcuvitz, *Radiation and Scattering of Waves* (Wiley Interscience, New York, 2003).
[5] V. P. Drachev, V. A. Podolskiy, and A. V. Kildishev, Opt. Express **21**, 15048 (2013).
[6] P. V. Kapitanova, P. Ginzburg, F. J. Rodriguez-Fortuno, D. S. Filonov, P. M. Voroshilov, P. A. Belov, A. N. Poddubny, Y. S. Kivshar, G. A. Wurtz, and A. V. Zayats, Nat. Commun. **5**, 3226 (2014).
[7] S. Ishii, A. V. Kildishev, E. Narimanov, V. M. Shalaev, and V. P. Drachev, Laser Photon. Rev. **7**, 265 (2013).
[8] V. G. Veselago, Sov. Phys. Uspekhi **10**, 509 (1968).
[9] S. L. Molodtsov, S. V. Halilov, V. D. P. Servedio, W. Schneider, S. Danzenbacher, J. J. Hinarejos, M. Richter, and C. Laubschat, Phys. Rev. Lett. **85**, 4184 (2000).
[10] G. V. Eleftheriades and K. G. Balmain, *Negative-Refraction Metamaterials: Fundamental Principles and Applications* (Wiley and IEEE Press, New York, 2005).
[11] H. N. S. Krishnamoorthy, Z. Jacob, E. Narimanov, I. Kretzschmar, and V. M. Menon, Science **336**, 205 (2012).
[12] C. L. Cortes, W. Newman, S. Molesky, and Z. Jacob, J. Optics **14**, 063001 (2012).
[13] S. Zhukovskiy, O. Kidwai, and J. E. Sipe, Opt. Lett. **36**, 2530 (2011).
[14] A. N. Poddubny, P. A. Belov, and Yu. S. Kivshar, Phys. Rev. A **84**, 023807 (2011).
[15] I. Iorsh, A. Poddubny, A. Orlov, P. Belov, and Yu. S. Kivshar, Phys. Lett. A **376**, 185 (2012).
[16] Q. Cheng, R. Liu, J. J. Mock, T. J. Cui, and D. R. Smith, Phys. Rev. B **78**, 121102 (2008).
[17] Z. Jacob, L. V. Alekseyev, and E. Narimanov, Opt. Exp. **14**, 8247 (2006).
[18] W. D. Newman, C. L. Cortes, and Z. Jacob, J. Opt. Soc. Am. B **30**, 766 (2013).
[19] A. V. Kabashin, P. Evans, S. Pastkovsky, W. Hendren, G. A. Wurtz, R. Atkinson, R. Pollard, V. A. Podolskiy, and A. V. Zayats, Nat. Mater. **8**, 867 (2009).
[20] R. M. A. Azzam and N. M. Bashara, *Ellipsometry and Polarized Light* (Elsevier Science Pub. Co., New York, 1987).
[21] A. V. Chshelokova, P. V. Kapitanova, A. N. Poddubny, D. S. Filonov, A. P. Slobozhanyuk, Yu. S. Kivshar, and P. A. Belov, J. Appl. Phys. **112**, 073116 (2012).
[22] A. Grbic and G. V. Eleftheriades, IEEE Trans. Antennas Propag. **51**, 2604 (2003).
[23] P. Alitalo, S. Maslovski, and S. Tretyakov, J. Appl. Phys. **99**, 064912 (2006).
[24] G. Gok and A. Grbic, IEEE Antennas Wireless Propag. Lett. **9**, 48 (2010).